

Applications of High-Resolution Electrospray Ionization Mass Spectrometry to Measurements of Average Oxygen to Carbon Ratios in Secondary Organic Aerosols

Adam P. Bateman,[†] Julia Laskin,[‡] Alexander Laskin,[§] and Sergey A. Nizkorodov^{*,†}

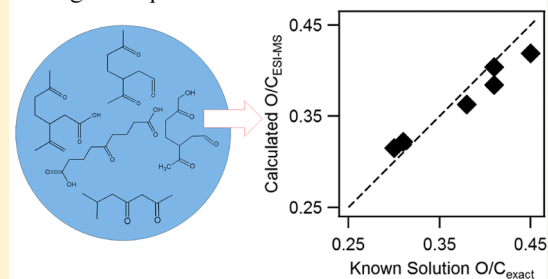
[†]Department of Chemistry, University of California, Irvine, California 92617, United States

[‡]Chemical and Materials Sciences Division and [§]Environmental Molecular Sciences Laboratory, Pacific Northwest National Laboratory, Richland, Washington 99352, United States

S Supporting Information

ABSTRACT: The applicability of high-resolution electrospray ionization mass spectrometry (HR ESI-MS) to measurements of the average oxygen to carbon ratio (O/C) in secondary organic aerosols (SOAs) was investigated. Solutions with known average O/C containing up to 10 standard compounds representative of low-molecular-weight SOA constituents were analyzed and the corresponding electrospray ionization efficiencies were quantified. The assumption of equal ionization efficiency commonly used in estimating O/C ratios of SOAs was found to be reasonably accurate. We found that the accuracy of the measured O/C ratios increases by averaging the values obtained from both the positive and negative modes. A correlation was found between the ratio of the ionization efficiencies in the positive (+) and negative (−) ESI modes and the octanol–water partition constant and, more importantly, the compound's O/C. To demonstrate the utility of this correlation for estimating average O/C values of unknown mixtures, we analyzed the ESI (+) and ESI (−) data for SOAs produced by oxidation of limonene and isoprene and compared them online to O/C measurements using an aerosol mass spectrometer (AMS). This work demonstrates that the accuracy of the HR ESI-MS method is comparable to that of the AMS with the added benefit of molecular identification of the aerosol constituents.

Average Composition Measured with HR ESI-MS



INTRODUCTION

Due to the molecular complexity inherent to secondary organic aerosols (SOAs), average properties such as the O/C ratio, H/C ratio, and/or carbon oxidation state (OS_c) have been used to characterize their aging/evolution in the atmosphere and laboratory.^{1–4} The time-of-flight aerosol mass spectrometer (ToF-AMS), with a mass resolution ($m/\Delta m$) of ~ 5000 ,⁵ and its low-resolution predecessor AMS⁶ are commonly used for measuring the average H/C and O/C ratios of SOAs in both field and laboratory studies.^{3,7–10} Recently, many studies of SOAs and environmental samples, including atmospheric particulate matter,^{11–13} atmospheric waters,^{14,15} biomass burning aerosol,^{16–18} and laboratory-generated aerosols,^{4,19–26} have utilized high-resolution ($m/\Delta m > 50000$) electrospray ionization mass spectrometry (HR ESI-MS) to provide both the average elemental ratios (H/C and O/C) and molecular level identification of individual constituents.

At the heart of this technique is the ESI process, which transfers dissolved analytes into the gas phase and ionizes them with minimal fragmentation, but with greatly varying ionization efficiency for different classes of compounds.²⁷ At sufficiently low concentrations, the ion abundances (i.e., peak intensities) in the ESI mass spectrum are proportional to the molar

concentrations (C_i), which are in turn proportional to the corresponding molar fractions (x_i) in the mixture:

$$\text{abundance}_i = \alpha_i C_i = \alpha_i x_i C_{\text{total}} \quad (1)$$

where α_i is the electrospray ionization (ESI) efficiency, which can vary significantly among different types of analytes.^{28,29} There have been a number of studies focused on the forward prediction of ESI efficiencies from a variety of molecular parameters, including molecular weight, molecular volume, molecular structure, pK_a , gas-phase proton affinity, gas-phase basicity, nonpolar surface area, surface activity, and octanol–water partition constant.^{24,29–40} For organic molecules, the octanol–water partitioning, surface activity, and nonpolar surface area appear to be the most useful metrics for predicting ESI responses.^{28,30,31} In general, amphiphilic molecules containing both nonpolar structural domains and easily ionizable functional groups (carboxylic acids, amines, amides, sulfonic acids, etc.) have the largest ESI efficiencies.

Received: April 30, 2012

Revised: June 27, 2012

Accepted: July 2, 2012

Published: July 2, 2012

Table 1. Compounds and Used in HR ESI-MS Experiments, Evaluation of the ESI Efficiency, Measurements of the O/C Ratios, and AMS Intercomparison^a

| standard compound | formula | MW (g/mol) | O/C ratio | mix A | mix B | mix C | mix D | mix E | mix F |
|---------------------------|--|------------|-----------|-------|-------|-------|-------|-------|-------|
| succinic acid | C ₄ H ₆ O ₄ | 118.09 | 1.00 | 0.2 | 0.02 | 2 | | | |
| DL-malic acid | C ₄ H ₆ O ₅ | 134.09 | 1.25 | 0.4 | 0.06 | 4 | | | |
| 6-methyl-2,4-heptanedione | C ₈ H ₁₄ O ₂ | 142.20 | 0.25 | 3 | 10 | 1 | 3 | 10 | 1 |
| 7-oxooctanoic acid | C ₈ H ₁₄ O ₃ | 158.19 | 0.38 | 5 | 3 | 3 | 5 | 4 | 1 |
| cis-pinonic acid | C ₁₀ H ₁₆ O ₃ | 184.23 | 0.30 | 2 | 2 | 1 | 2 | 10 | 1 |
| cis-pinic acid | C ₉ H ₁₄ O ₄ | 186.21 | 0.44 | 1 | 1 | 1 | 1 | 1 | 0.7 |
| azelaic acid | C ₉ H ₁₆ O ₄ | 188.22 | 0.44 | 1 | 0.4 | 0.4 | 7 | 2 | 2 |
| citric acid | C ₆ H ₈ O ₇ | 192.12 | 1.17 | | | | 0.1 | 0.1 | 1 |
| camphoric acid | C ₁₀ H ₁₆ O ₄ | 200.23 | 0.40 | | | | 0.8 | 0.2 | 8 |
| 5-oxoazelaic acid | C ₉ H ₁₄ O ₅ | 202.20 | 0.56 | 2 | 0.4 | 2 | 4 | 1 | 5 |
| average O/C ratio | | | | 0.41 | 0.30 | 0.59 | 0.42 | 0.32 | 0.49 |

^aThe concentrations ($\times 10^{-5}$ M) of each compound in mixtures A–F before dilution are listed.

Table 2. Additional Compounds and Their Mixtures Used for the HR ESI-MS O/C Analysis^a

| standard compound | formula | MW (g/mol) | O/C ratio | mix G | mix H | mix I | mix J | mix K | mix L |
|---------------------------|--|------------|-----------|-------|-------|-------|-------|-------|-------|
| 6-methyl-2,4-heptanedione | C ₈ H ₁₄ O ₂ | 142.20 | 0.25 | 3 | 10 | 1 | 3 | 10 | 1 |
| 7-oxooctanoic acid | C ₈ H ₁₄ O ₃ | 158.19 | 0.38 | 5 | 3 | 3 | 5 | 4 | 1 |
| cis-pinonic acid | C ₁₀ H ₁₆ O ₃ | 184.23 | 0.30 | 2 | 2 | 1 | 2 | 10 | 1 |
| cis-pinic acid | C ₉ H ₁₄ O ₄ | 186.21 | 0.44 | 1 | 1 | 1 | 1 | 1 | 0.7 |
| azelaic acid | C ₉ H ₁₆ O ₄ | 188.22 | 0.44 | 1 | 0.4 | 0.4 | 7 | 2 | 2 |
| camphoric acid | C ₁₀ H ₁₆ O ₄ | 200.23 | 0.40 | | | | 0.8 | 0.2 | 8 |
| 5-oxoazelaic acid | C ₉ H ₁₄ O ₅ | 202.20 | 0.56 | 2 | 0.4 | 2 | 4 | 1 | 5 |
| average O/C ratio | | | | 0.38 | 0.30 | 0.41 | 0.41 | 0.31 | 0.45 |

^aThe concentrations ($\times 10^{-5}$ M) of each compound in mixtures G–L before dilution are listed.

The ESI response is further complicated by a competition for charge between different analyte molecules. As a result, the ionization efficiency may be dependent on the concentrations of other compounds present in solution (matrix effects).^{27,28,35,41} Such inherent complications to the ESI method make quantitative analysis of unknown mixtures challenging, especially without a priori knowledge of the types of compounds present in the mixture. Due to the lack of information about the ESI efficiencies, many previous studies reporting elemental ratios for SOAs obtained by the HR ESI-MS method had to assume the same values of α_i for all detectable compounds.^{4,11,19,21–23,26,42} Hall and Johnston were able to achieve more quantitative results in HR ESI-MS analysis of α -pinene SOA using standard additions of known SOA constituents (pinonic acid and pinic acid) and assuming that the other monomer products had a similar ESI efficiency.⁴³

The goal of this work is to evaluate the accuracy of the assumption that SOA constituents have equal ESI efficiency factors, α_i , for the purpose of measuring the average O/C ratio in SOA. This is accomplished through HR ESI-MS experiments with aqueous solutions of atmospherically relevant organic molecules mixed in predefined proportions. We show that the average O/C ratios calculated assuming equal ESI efficiencies are in reasonable agreement with the known O/C of the premixed solutions. We find that the ESI response can be correlated with a compound's log P value (P is an octanol–water partition constant) or the equilibrium ratio of a compound's concentration in nonpolar (octanol) and polar (water) solvents, which in turn is related to a compound's O/C ratio. This correlation makes it possible to improve the accuracy of the O/C estimation from HR ESI-MS measurements. We show that the accuracy of these estimates is comparable to that of the AMS method, thus offering a method

to evaluate average atomic ratios in SOA material while retaining the molecular information about the material's constituents.

MATERIALS AND METHODS

Standard solutions containing up to 10 different organic compounds were prepared in acetonitrile (HPLC grade). Acetonitrile was the preferred solvent over water or methanol for this study due to its enhanced ESI performance²⁸ and because it does not react with the test compounds or SOAs.²⁰ In addition, many of the organic test compounds were not soluble in water. It has been previously reported that the ESI mass spectra from SOAs extracted in water or acetonitrile are quite similar.¹⁹ Test compounds used in this study included DL-malic acid (Sigma-Aldrich, 99% stated purity), succinic acid (Sigma-Aldrich, 99%), 6-methyl-2,4-heptanedione (Acros Organics, 98%), 7-oxooctanoic acid (Sigma-Aldrich, 98%), azelaic acid (Sigma-Aldrich, 98%), 5-oxoazelaic acid (Sigma-Aldrich, 96%), cis-pinonic acid (Sigma-Aldrich Library of Rare Chemicals), cis-pinonic acid (Sigma-Aldrich, 98%), citric acid (Fluka Analytical, 99.5%), and camphoric acid (Sigma-Aldrich, 99%). All compounds were used as received without additional purification.

Multifunctional organic acids and a diketone compound were chosen to represent the SOA constituents. Previous work by the authors using HR-ESI-MS found that ~55% of the peaks in limonene SOA contain a carboxyl group and more than 40% of the compounds have a carbonyl group.²⁰ Two test compounds, pinonic acid and pinic acid, have been previously detected in α -pinene SOA using GC–MS; that study also attributed a substantial fraction of the particulate mass to organic acids.⁴⁴ Pinonic acid and pinic acid along with a variety of other multifunctional organic acids have been detected in ambient air

Table 3. Relative ESI Efficiency of Each Standard Compound Averaged across All the Dilutions and Mixtures for Each Ionization Mode^a

| standard compound | (+) ES mode | (-) ES mode | (+)/(−) ratio |
|---------------------------|-------------------------------|-------------|-------------------------------|
| succinic acid | 0.2 ± 0.8 | 3.0 ± 20.0 | 0.07 ± 0.6 |
| DL-malic acid | 0.1 ± 0.5 | 10.0 ± 8.0 | 0.01 ± 0.09 |
| 6-methyl-2,4-heptanedione | 0.1 ± 2.0 | 0.02 ± 0.1 | 9.0 ± 100.0 |
| 7-oxooctanoic acid | 4.0 ± 20.0 | 1.0 ± 6.0 | 4.0 ± 30.0 |
| cis-pinonic acid | 1.0 ± 7.0 | 2.0 ± 10.0 | 0.4 ± 4.0 |
| cis-pinic acid | 0.06 ± 0.3 | 1.0 ± 5.0 | 0.07 ± 0.5 |
| azelaic acid | 2.0 ± 20.0 | 2.0 ± 20.0 | 1.0 ± 10.0 |
| citric acid | (4.0 ± 20) × 10 ^{−5} | 4.0 ± 30.0 | (6.0 ± 40) × 10 ^{−6} |
| camphoric acid | 0.2 ± 1.0 | 1.0 ± 5.0 | 0.2 ± 10.0 |
| 5-oxoazelaic acid | 1.0 ± 8.0 | 1.0 ± 7.0 | 1.0 ± 10.0 |

^aEach compound's ESI efficiency has been scaled relative to that of (+) mode *cis*-pinonic acid. The ratio of (+) mode ESI efficiency to (−) mode ESI efficiency is also listed.

above forests.⁴⁵ In addition, multifunctional acids have been identified in SOAs formed from different monoterpenes.⁴⁶ Therefore, the use of multifunctional carboxylic acids for the test compounds is relevant for extrapolation to SOAs formed via oxidation of monoterpenes.

Even though the number of test compounds selected for this study is not very large, we compensated for this by (1) studying them over a significant range of concentrations and (2) mixing these compounds in a number of different ways. Stock solutions were prepared for all compounds with concentrations ranging from 10^{−5} to 10^{−3} M. Aliquots of 5–500 μL of each stock solution were mixed and further diluted with acetonitrile to produce standard mixtures of known composition as listed in Tables 1 and 2 with total organic content (*C*_{total}) on the order of ~10^{−4} M. Each standard mixture was further diluted with acetonitrile to create two less concentrated standards with total concentrations *C*_{total} of ~10^{−6} and ~10^{−8} M. Two sets of solutions were created: mixtures A–F contained compounds with a larger spread of molecular sizes and structures (Table 1), and mixtures G–L contained compounds that were more similar in structure (Table 2). Mixtures G–L used the same compounds as mixtures A–F with the exception of citric acid, DL-malic acid, and succinic acid.

HR ESI-MS analysis was performed on all mixtures A–F and G–L at all levels of dilution (*C*_{total} ≈ 10^{−4}, 10^{−6}, and 10^{−8} M). At least two mass spectra were recorded for each sample, as outlined in Table S1 of the Supporting Information. The mass spectra were obtained using an LTQ (linear ion trap)–Orbitrap hybrid mass spectrometer (Thermo Electron Corp., Inc.) with a modified ESI source. Solutions were directly injected through a pulled fused silica capillary tip at a flow rate of 1 μL/min with no additives used to enhance ionization. The capillary voltage was between 2 and 3 kV. The instrument was operated in both (+) and (−) ionization modes with a mass resolving power *m*/*Δm* = 60000 at *m/z* 400 sufficient to resolve all the compounds probed in this study. Mass calibrations were performed using a standard calibration mix, MSCAL 5 (Sigma-Aldrich, Inc.). Mass spectra acquired from all mixtures in positive and negative modes were first converted to their neutral precursor's molecular weight (mass of Na⁺ subtracted for (+)-mode ions and mass of H⁺ added for (−)-mode ions) and then aligned along a common molecular weight axis. The background peaks appearing in the solvent mass spectra were removed from all mass spectra. For SOA samples, molecular formulas, C_{*c*}H_{*h*}O_{*o*}, were assigned to the neutral precursors on the basis of the accurate mass measurements for their ions, as has been

described previously.⁴ The analysis performed herein was only conducted for CHO compounds; its applicability for N- and/or S-containing compounds will be explored in future studies.

Following peak identification, average atomic ratios were calculated from both the known molar fractions *x_i* and the HR ESI-MS ion abundances as follows:

$$O/C_{\text{exact}} = \sum_i x_i o_i / \sum_i x_i c_i \quad (2)$$

$$O/C_{\text{weighted}} = \sum_i (\text{abundance}_i) o_i / \sum_i (\text{abundance}_i) c_i \quad (3)$$

$$O/C_{\text{unweighted}} = \sum_i o_i / \sum_i c_i \quad (4)$$

For the remainder of this paper, we will use the letters *c*, *h*, and *o* to refer to the number of C, H, and O atoms, respectively, in the individual molecules. We will use O/C to refer to the average atomic ratio of an entire mixture. Equation 2 provides the actual values for the average O/C elemental ratio in the tested mixtures, as listed in Tables 1 and 2. Variations in the composition of mixtures A–F were designed to span a range of O/C from 0.30 to 0.59, while mixtures G–L had O/C ratios ranging from 0.3 to 0.45. Both sets of mixtures overlap well with the O/C values measured for SOAs in chamber studies.^{4,11,19,21,23}

If the electrospray ionization efficiency for each compound were known and all the compounds present in the mixture were above the detection limit, one could use the measured ion abundances and eq 1 to obtain the exact O/C from the ESI mass spectra. In practice, this will not be exact for solutions containing undetectable compounds such as saturated hydrocarbons. However, this assumption should be valid for the test mixtures used in this work because every compound is detectable and its detection sensitivity is quantified. In contrast, ESI efficiencies are generally not known for each of the components of a complex mixture such as SOA. Equations 3 and 4 reflect the assumptions made in previous work on SOA analysis using ESI-MS. Equation 3 calculates O/C assuming that all ESI efficiencies are equal, and therefore, the O/C ratios of the individual molecules are weighted by the corresponding measured ion abundances (i.e., the relative peak areas or heights in the mass spectrum).^{4,19,21,23,26} Equation 4 calculates the average O/C without any abundance weighting using only the detected compound's *o/c*.^{11,22,42,47}

The O/C values measured with HR ESI-MS and the ToF-AMS were compared using mixtures A–F. The standard mixtures were atomized into a clean 300 L Teflon chamber. The generated aerosols passed through a series of four diffusion dryers before being sampled by an AMS instrument (Aerodyne, ToF-AMS with mass resolving power $m/\Delta m \approx 5000$). The O/C_{measured} values were calculated for the positive ion mode AMS spectra following the procedures described by Aiken et al.^{9,10} Additional corrections were made to the O/C ratios calculated using the AMS software Analytical Procedure for Elemental Separation (APES) using $(\text{CO}^+)_{\text{org}}/(\text{CO}_2^+)_{\text{org}}$ and $(\text{H}_2\text{O}^+)_{\text{org}}/(\text{CO}_2^+)_{\text{org}}$ values calculated from each individual experiment, as described by Chen et al.⁴⁸ The values used in this work are tabulated in Table S2 of the Supporting Information.

RESULTS AND DISCUSSION

Correlations between Electrospray Ionization Efficiencies and Molecular Properties. The ESI efficiency factors were calculated for each test compound by dividing the measured ion abundance by the corresponding known molar fraction per eq 1. The measured ion abundances corresponded to the deprotonated molecules, $[\text{M} - \text{H}]^-$, in the (–) ESI mode and to sodiated $[\text{M} + \text{Na}]^+$ molecules in the (+) ESI mode. The ESI efficiency values of each compound averaged across all mixtures A–L and normalized to the ionization efficiency value obtained for *cis*-pinonic acid in the (+) mode are listed in Table S3 of the Supporting Information. The ESI efficiencies in the (+) and (–) modes are not directly comparable, as the ionization mechanisms differ (complexation with Na^+ in the (+) mode and deprotonation in the (–) mode).

The ESI efficiency values obtained for the same compound from all mixtures at different dilution levels were averaged together, and the results are listed in Table 3. While the ESI efficiency values vary by many orders of magnitude from the different dilution levels, the variance of the (+)/(–) ratio is much smaller, the values remaining within 1 order of magnitude (Table S3, Supporting Information). There is also a large degree of variation in the observed ESI efficiencies for different compounds within a given ESI mode reaching several orders of magnitude (Table 3). The spread is especially wide in the (+) ESI mode. The (–) ESI efficiencies are of a similar magnitude for all compounds except for 6-methyl-2,4-heptanedione, the only compound that is lacking a carboxylic acid group. The ionization efficiencies of carboxylic acids in the (–) ESI mode are expected to be comparable because of the relative ease of deprotonation of the carboxyl group.

The octanol–water partition constant (usually reported as its natural logarithm, $\log P$) is an equilibrium ratio of concentrations of the compounds distributed between octanol (nonpolar) and water (polar) phases. It is a convenient measure of a compound's polarity, as large $\log P$ values tend to be attributed to extended nonpolar regions and small $\log P$ values are attributed to highly polar groups.⁴⁹ Figure 1a explores the correlation between the relative ESI efficiency factors and calculated $\log P$ values (the $\log P$ values are tabulated in Table S4 of the Supporting Information). Although the data are quite scattered, the (+) ESI efficiencies increase with $\log P$, while the (–) ESI efficiencies decrease with $\log P$. Previous studies have found an increase of the (–)-mode ESI efficiency with $\log P$ using mainly aromatic compounds with $\log P$ values >1.5 .^{24,41} The $\log P$ values used in this work ranged from -1.7 to $+1.8$.

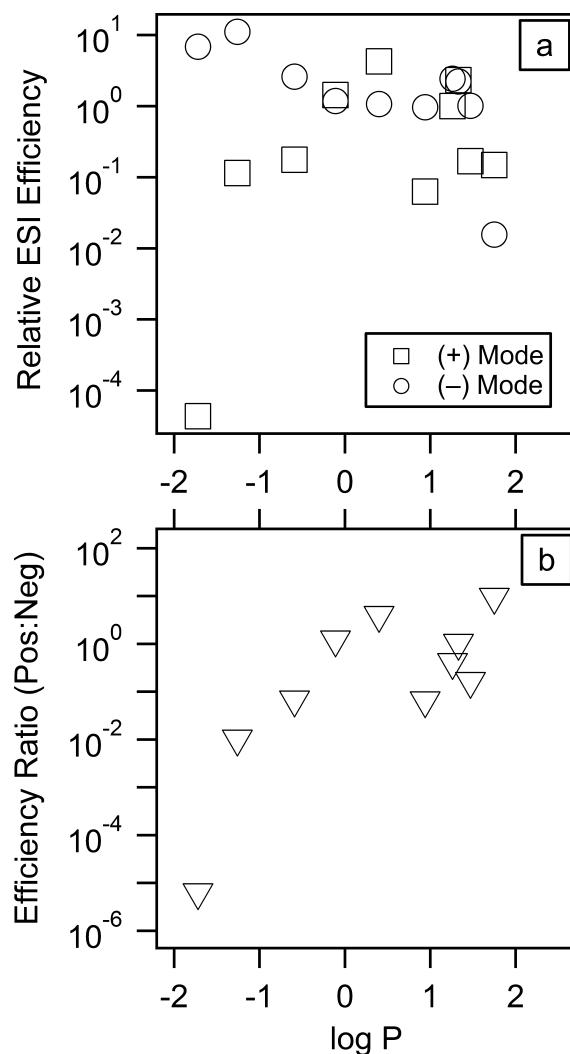


Figure 1. $\log P$ values calculated for each standard compound and plotted against (a) the average ESI efficiency factor for both ESI modes scaled relative to that of (+) mode *cis*-pinonic acid ($\log P = 1.26$) and (b) the ratio of (+) mode ESI efficiency to (–) mode ESI efficiency. The relative ESI efficiencies for both ESI modes are uncertain to within a factor of 2, as estimated from comparing results for multiple mixtures and samples. The efficiency ratios are uncertain to within a factor of 10.

There is a more obvious correlation between $\log P$ and the ratio of (+) ESI mode and (–) ESI mode ionization efficiencies (Figure 1b). The data suggest that compounds with high $\log P$ values have larger ionization efficiencies in the (+) mode and compounds with low $\log P$ values have larger ionization efficiencies in the (–) ESI mode. Thus, the largest ESI efficiency ratio and largest $\log P$ value correspond to 6-methyl-2,4-heptanedione, which is barely detectable in the (–) mode, and the smallest ESI efficiency ratio and smallest $\log P$ value correspond to citric acid, only detected in the (+) mode at the highest concentrations.

Average Atomic Ratios of Test Organic Mixtures.

Figure 2 displays the calculated O/C as a function $\text{O/C}_{\text{exact}}$ as calculated from eq 2 using the known molar concentrations of the test solutions. The $\text{O/C}_{\text{unweighted}}$ values as calculated by eq 4 are shown in Figure 2a and b, while the $\text{O/C}_{\text{weighted}}$ values as calculated from eq 3 are shown in Figure 2c and d. Data for mixtures A–F and G–L are shown in the left-hand panels and

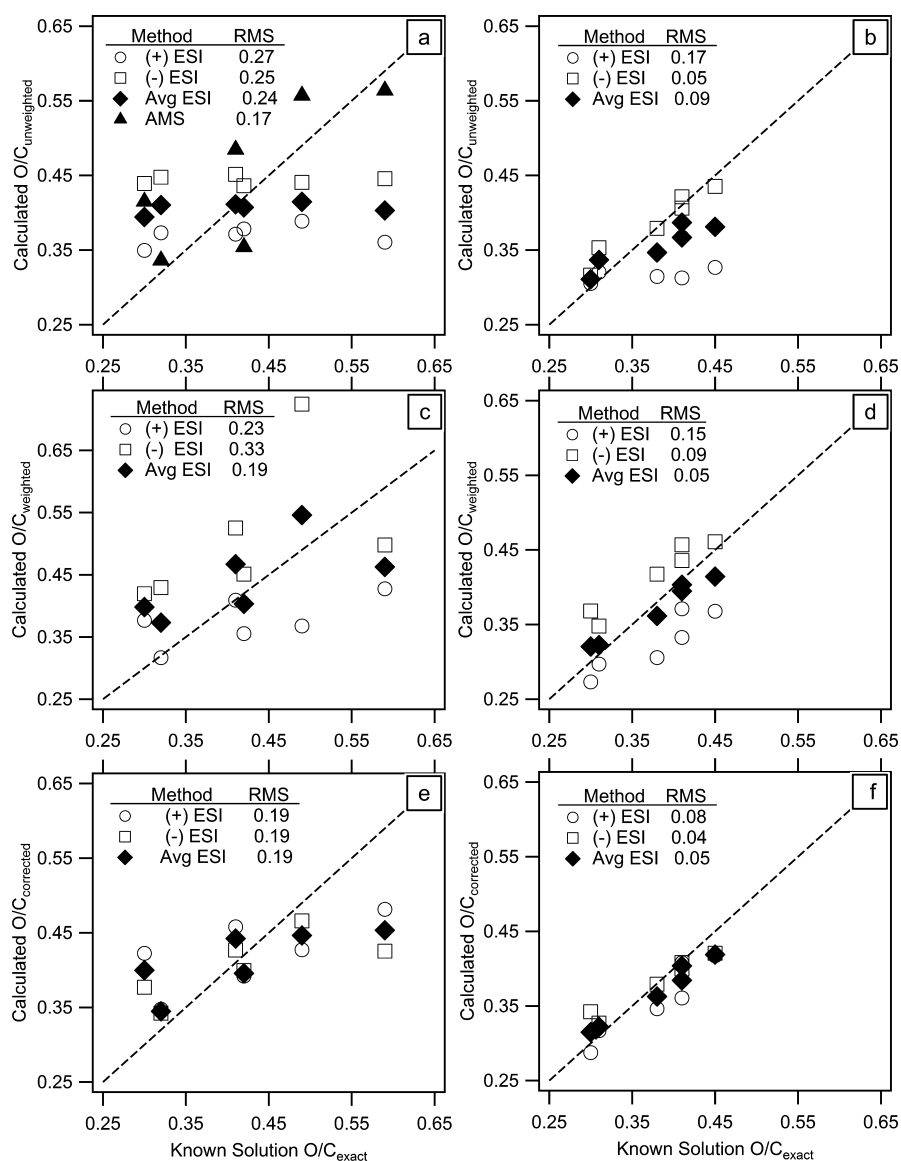


Figure 2. (a) Unweighted O/C calculated from ESI spectra plotted against each solution's O/C_{exact} value for mixtures A–F as listed in Table 1. (b) Same for mixtures G–L from Table 2. (c) Abundance-weighted O/C calculated from ESI spectra for mixtures A–F. (d) Same for mixtures G–L. (e) ESI efficiency corrected abundance-weighted O/C calculated from ESI spectra for mixtures A–F. (f) Same for mixtures G–L. Different markers refer to the positive ion mode (open circles), the negative ion mode (open squares), and the average of the two modes (solid diamonds). AMS O/C ratios (solid triangles in panel a) were calculated only in the positive ion mode for mixtures A–F. The standard deviation for the O/C_{corrected} values from multiple measurements/samples, propagated through the calculation, was estimated as ± 0.2 O/C unit. The root-mean-square (rms) values as calculated from the differences between the calculated and actual O/C values for each data set are tabulated in each panel.

right-hand panels, respectively. The O/C values were calculated for mass spectra obtained from the (+) mode, the (–) mode, the average of the (+) and (–) modes, and the ToF-AMS data (Figure 2a only). Figure 2 demonstrates that, on the whole, the O/C measurements achieve a reasonable degree of accuracy. The HR ESI-MS estimates appear to have accuracy comparable to that of the AMS results (Figure 2a). The HR ESI-MS estimates display a clear trend toward overpredicting at low O/C values and underpredicting the O/C values as O/C increases; such a trend is less apparent in the AMS data. The O/C ratios calculated from the (+) mode ESI spectra are uniformly smaller than the corresponding values calculated from the (–) mode ESI spectra. This is a reflection of the fact that for the compounds examined in this study the (–) mode tends to

ionize molecules with higher *o/c* more efficiently than the (+) mode.

The use of ion abundance as the weighting factor when calculating the O/C appears to slightly enhance the accuracy and lessen the apparent skew in detection of higher *o/c* ratio compounds in both ESI modes (compare panels a and c and panels b and d of Figure 2). On the basis of the results shown in Figure 2a–d, it can be concluded that the most accurate prediction of solution O/C ratios comes from averaging the O/C ratios measured from both (+) and (–) ESI modes. The use of abundance weighting on the average O/C values enhances the accuracy in all cases. It should be noted that the molecules chosen as standards in this study represent only a small subset of possible constituents in atmospheric SOAs, and the degree of accuracy for estimating the average O/C in SOAs will decrease

as the molecular complexity increases, as demonstrated between mixtures A–F and G–L, panels a, c, and e vs panels b, d, and f of Figure 2. In addition, the better agreement of averaging both ESI modes may be due to cancellation of errors, rather than an improvement in accuracy. Nevertheless, a more thorough assessment of the solution O/C can be achieved through a combination of data from both ionization modes and therefore the ability to detect a larger set of constituent molecules.

Parametrizing ESI Efficiencies with Molecular o/c .

While the correlation between the ESI efficiency and $\log P$ is informative, it is not especially useful for the analysis of complex SOA samples containing unknown compounds. Analysis of HR ESI-MS data typically returns a long list of formulas for all the detected (and assignable) compounds but provides no structural information, which is necessary for determination of a compound's $\log P$. Therefore, we explored a correlation between the o/c values of the individual compounds and their relative ESI efficiencies. In addition to the test compounds listed in Table 1, we also included data for the major peaks observed in mass spectra of limonene SOA from previous work.^{4,19,26} The specific limonene oxidation products and their predicted $\log P$ values are included in Table S5 of the Supporting Information. The structures included in Table S5 are based on previous identification of compounds in limonene SOA using GC-MS.^{46,50} In some cases more than one structure was identified with the same molecular formula and exact compound mass; in such a case, the $\log P$ values were averaged together.

The o/c values of both the test compounds and limonene SOA constituents were strongly correlated to $\log P$ (Figure 3a) and to the ratio of their (+) and (–) mode ionization

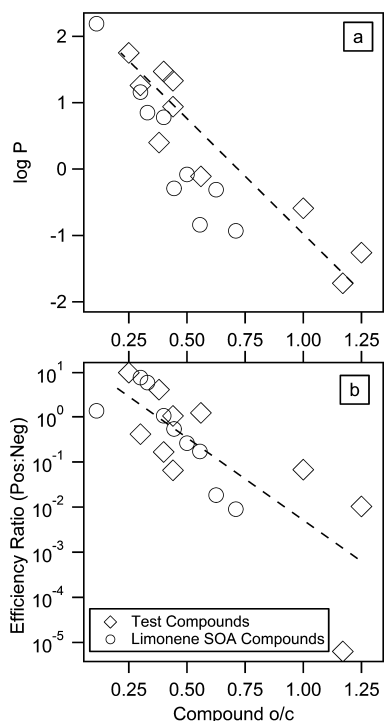


Figure 3. Compound o/c ratio plotted against (a) the compound's $\log P$ and (b) the ratio of (+) ESI efficiency to (–) ESI efficiency for each compound. The fit in panel b was calculated using eq 5. The uncertainty in the efficiency is on the order of a factor of 10.

efficiencies (Figure 3b). The o/c values of the individual compounds were less correlated with their (+) or (–) ESI mode ionization efficiencies, as seen in Figure S1 of the Supporting Information. The best fit line for the correlation shown in Figure 3b can be described by the equation

$$\log\left(\frac{\alpha_{\text{ESI}(+)}}{\alpha_{\text{ESI}(-)}}\right) = (\text{slope})\frac{o}{c} + \text{const} \quad (5)$$

The intercept in eq 5 has no physical meaning since the ratio of ESI efficiencies is arbitrarily normalized. The determined slope was -8.4 and -10 for the test compounds and the known compounds in limonene SOA, respectively. The negative sign of the slope reflects the fact that compounds with high o/c values (such as carboxylic acids) are easier to detect in the (–) mode relative to compounds with low o/c values. We should stress that the specific value of the slope depends on the instrument settings used during the experiments and quite possibly on the types of compounds in the mixture. Separate parametrizations must be constructed for the unknown mixtures analyzed using different ESI instrument settings.

To test the effectiveness of the relationship in eq 5, we used the set of compounds with known ESI efficiencies from mixtures A–F and G–L. Combining eqs 1 and 3 gives

$$O/C_{\text{corrected}} = \frac{\sum_i \left(\frac{\text{abundance}_i}{\alpha_i} o_i \right)}{\sum_i \left(\frac{\text{abundance}_i}{\alpha_i} c_i \right)} \quad (6)$$

The summation in eq 6 extends over all molecules which can be assigned to molecular formulas from the HR ESI-MS accurate mass measurements. The ion abundances, number of carbon atoms, and number of oxygen atoms in each molecule are experimentally determined quantities. We can then parametrize the relative ESI efficiencies for each ESI mode as a function of the individual molecules' o/c ratios as follows:

$$\log[\alpha_i^{\text{positive}}] = k_{\text{positive}} \frac{o_i}{c_i} \quad (7)$$

$$\log[\alpha_i^{\text{negative}}] = k_{\text{negative}} \frac{o_i}{c_i} \quad (8)$$

The multiplication factors in eqs 7 and 8 were fitted explicitly from the (+) and (–) ESI mode data, and the results of the test compounds were $k_{\text{positive}} = -5.1$ and $k_{\text{negative}} = 3.3$. The difference in the coefficients, $k_{\text{positive}} - k_{\text{negative}}$, was fixed to slope = -8.4 dictated by the correlation expressed by eq 5. With these parametrizations in hand, the $O/C_{\text{corrected}}$ can be calculated using eq 6 for all mixtures A–F and G–L. Panels e and f of Figure 2 show the $O/C_{\text{corrected}}$ values plotted versus the O/C_{exact} for mixtures A–F and G–L, respectively. This parametrization reduces the difference in O/C calculated from the (+)- and (–)-mode ESI data, in addition to increasing the accuracy of the calculated O/C values.

Applications to O/C Measurements of SOAs. To test the applicability of this parametrization to the analysis of unknown mixtures, a set of mass spectra for SOA samples obtained from dark ozonolysis of *d*-limonene was used.²⁶ SOA was prepared at different initial *d*-limonene mixing ratios in a smog chamber, collected on a filter, extracted in acetonitrile, and examined with HR ESI-MS. The AMS was directly connected to the chamber during the SOA experiments at the low mass loadings and recorded the O/C ratios. The O/

C_{weighted} values calculated using eq 3 for all SOA samples are plotted in Figure 4 as a function of the initial *d*-limonene

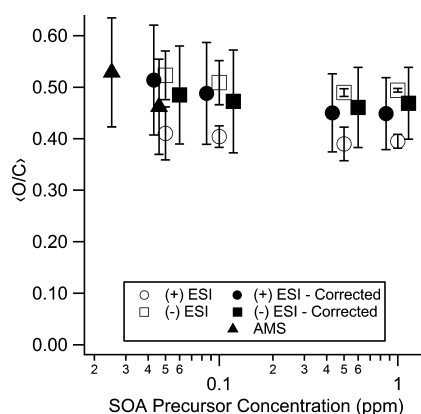


Figure 4. Average O/C values calculated for limonene SOA at different precursor concentrations in the smog chamber. The O/C_{weighted} values (open symbols) and $O/C_{\text{corrected}}$ values (solid symbols) were calculated for both the (+) mode (circles) and the (-) mode (squares). The O/C ratios were calculated from AMS data using the procedure as outlined by Aiken et al.⁹ with APES corrections as outlined by Chen et al.⁵⁴ (closed triangles). Error bars were estimated from comparing multiple samples for the (+) ESI and (-) ESI data sets and using an error of $\pm 90\%$ for the ESI efficiencies. Error bars on the AMS data set were assumed to be 20%. The SOA precursor concentrations for each cluster of points were the same (0.05, 0.1, 0.5, and 1 ppm), but have been offset in this figure for clarity in viewing the error bars.

mixing ratio (open circles and squares). Four separate mixing ratios of SOA precursors (0.05, 0.1, 0.5, and 1 ppm) were used for the SOA preparation; however, the data are spread out along the mixing ratio axis for clarity in viewing the error bars. Error bars were calculated from multiple samples using an estimated error in the relative ESI efficiencies of $\pm 90\%$ (i.e., we assume that the relative ionization efficiencies are known to within 1 order of magnitude). The resulting errors in O/C (listed in Table S6 of the Supporting Information) are on the order of ± 0.1 O/C unit. There is a significant difference between the average O/C values calculated from the ESI (+) data ($O/C \approx 0.40$) and ESI (-) data ($O/C \approx 0.50$).

The ESI efficiency factors are unknown for the individual SOA compounds, and the correlation of the ratio of the (+) and (-) ESI efficiencies with o/c (eq 5) cannot be easily converted into the separate correlations as done for the known compounds (eqs 7 and 8). Therefore, k_{positive} and k_{negative} in eqs 7 and 8 were treated as adjustable parameters chosen to provide the best match between the corrected O/C values calculated from the ESI (+) and (-) mode data. The values that fit the limonene SOA data set were $k_{\text{positive}} = -7$ and $k_{\text{negative}} = 3$ (note that the difference in the factors was constrained to slope = -10, the value based on the correlation for the known limonene SOA compounds). The $O/C_{\text{corrected}}$ values calculated from these parametrizations are shown in Figure 4 (solid symbols). The $O/C_{\text{corrected}}$ calculated from the (+) ESI mode and (-) ESI mode data agree well with each other (~ 0.48) and likely represent a better approximation to the true O/C in limonene SOA. Also plotted in Figure 4 are the O/C values obtained from online chamber measurements using the AMS methods. The O/C values (0.46–0.53) obtained from the AMS data using the procedure of Aiken et al.,^{9,10} as modified by

Chen et al.,⁴⁸ are in good agreement with the O/C values from the HR ESI-MS measurements. The O/C values from the AMS were not calculated for chamber experiments at the higher concentrations due to the very high particle mass loadings ($>300 \mu\text{g m}^{-3}$).

The method described above was also applied to an HR ESI-MS data set obtained from the dark ozonolysis of isoprene.²¹ The O/C values obtained from HR ESI-MS analysis and AMS analysis are listed in Table S7 of the Supporting Information. In this case, the O/C values obtained from the (+) and (-) mode were quite similar to begin with. Specifically, $O/C_{\text{unweighted}}$ values were 0.56 and 0.60, and O/C_{weighted} values were 0.56 and 0.57, in the (+) and (-) modes, respectively. The ratio of (+) to (-) ESI abundances was plotted against each compound's o/c value and fit to eq 5, resulting in slope = -0.33. Unlike limonene SOA compounds, there is limited structural information for major isoprene SOA compounds. Therefore, the full distributions of compounds detected by both the (+) and (-) modes were used. The large difference between the values of the slope for the limonene and isoprene data sets is ascribed to differences in the instrument settings, as well as the types of compounds in the mixture. The k_{positive} and k_{negative} chosen in this case were -0.165 and 0.165, respectively, again constrained by the slope determined from eq 5. The corrected O/C ratios were 0.57 and 0.56 in the (+) and (-) modes, respectively.

The O/C value obtained from online AMS analysis of the isoprene chamber aerosol was 0.58, which is again in excellent agreement with the parametrization values obtained via ESI-MS. We note, however, that while the AMS and HR ESI-MS O/C values for the limonene and isoprene SOAs are in good agreement, it is not a conclusive validation of the parametrization technique. Ideally, the exact O/C values of the test SOAs would have been measured using elemental analysis techniques. Unfortunately, this is not an easy task in view of the significant material requirements (several milligrams) of such methods.

The molecular weights of the test compounds listed in Tables 1 and 2 ranged from 118 to 202, and those of the identified limonene SOA compounds (Table S5, Supporting Information) ranged from 138 to 202. The detectable SOA compounds spanned a wider range of molecular weights: 110–900 for limonene SOA and 100–800 for isoprene SOA. It is not clear whether the parametrization developed for the low molecular weight compounds can be extrapolated to the higher molecular weight compounds because their ESI efficiencies could in principle correlate differently to the o/c ratios. However, the parametrization was conducted using test compounds with a range of o/c values (0.25–1.25) similar to those for limonene SOA (0.1–0.9) and isoprene SOA (0.13–1.25). Therefore, as long as the primary ionization mechanisms for the low- and high-molecular-weight compounds are similar, the extrapolation should be reliable.

The parametrization method proposed in this study relies on the use of both positive and negative ionization modes and may be less useful for ambient samples containing compounds with functional groups that are susceptible to ionization in only one mode. In addition, ambient samples contain mixtures of inorganic and organic compounds. It is difficult to fully evaluate the possible effect of inorganic ions on the ionization of the SOA compounds. Most of the (+) ESI mode compounds observed in this work were detected as Na^+ adducts. If NH_4^+ or metal ions were present in the extracted ambient sample in

significant amounts, they could also form adducts with the SOA compounds during ionization.¹⁸ Metal complexation may be alleviated by desalting the extracted sample using solid-phase extraction techniques prior to the ESI-MS analysis, as done, for example, in the analyses of the dissolved organic matter in ocean water⁵¹ and for field-collected aerosol samples.⁵²

As the *o/c* ratio is obtained directly from the HR ESI-MS measurements and peak assignments, a priori knowledge of the composition is not necessary to apply the parametrization. As a proof of principle, we have applied this parametrization to chamber-generated SOAs and found good agreement with the commonly used AMS method of measuring the O/C ratio. As environmental HR ESI-MS measurements become more common,⁵³ parametrizations of this type have a great potential for improving the elemental analysis of SOA samples.

■ ASSOCIATED CONTENT

● Supporting Information

Tables giving the number of ESI mass spectra collected; parameters used for the AMS determination of the O/C ratio; relative ESI efficiency of each standard; structures, formulas, and calculated log *P* values for compounds used in analysis of the solution O/C; previously identified compounds in limonene SOA; O/C values estimated for SOA from the dark ozonolysis of limonene and from the dark ozonolysis of isoprene. Figure showing the correlation of the relative ionization efficiency with *o/c*. This material is available free of charge via the Internet at <http://pubs.acs.org>.

■ AUTHOR INFORMATION

Corresponding Author

*E-mail: nizkorod@uci.edu; phone: (949) 824-1262.

Notes

The authors declare no competing financial interest.

■ ACKNOWLEDGMENTS

The University of California, Irvine, group gratefully acknowledges support by National Science Foundation Grants ATM-0831518 and CHE-0909227. A.P.B. acknowledges support provided by the Department of Energy (DOE) Global Change Education Program. The Pacific Northwest National Laboratory (PNNL) group acknowledges support from the intramural research and development program of the W. R. Wiley Environmental Molecular Sciences Laboratory (EMSL). EMSL is a national scientific user facility located at PNNL and sponsored by the Office of Biological and Environmental Research of the United States. PNNL is operated for the U.S. DOE by Battelle Memorial Institute under Contract DE-AC06-76RL0 1830.

■ REFERENCES

(1) Kroll, J. H.; Donahue, N. M.; Jimenez, J. L.; Kessler, S. H.; Canagaratna, M. R.; Wilson, K. R.; Altieri, K. E.; Mazzoleni, L. R.; Wozniak, A. S.; Bluhm, H.; Mysak, E. R.; Smith, J. D.; Kolb, C. E.; Worsnop, D. R. Carbon oxidation state as a metric for describing the chemistry of atmospheric organic aerosol. *Nat. Chem.* **2011**, *3* (2), 133–139.

(2) Ng, N. L.; Canagaratna, M. R.; Zhang, Q.; Jimenez, J. L.; Tian, J.; Ulbrich, I. M.; Kroll, J. H.; Docherty, K. S.; Chhabra, P. S.; Bahreini, R.; Murphy, S. M.; Seinfeld, J. H.; Hildebrandt, L.; Donahue, N. M.; DeCarlo, P. F.; Lanz, V. A.; Prevot, A. S. H.; Dinar, E.; Rudich, Y.; Worsnop, D. R. Organic aerosol components observed in Northern

Hemispheric datasets from aerosol mass spectrometry. *Atmos. Chem. Phys.* **2010**, *10* (10), 4625–4641.

(3) Jimenez, J. L.; Canagaratna, M. R.; Donahue, N. M.; Prevot, A. S. H.; Zhang, Q.; Kroll, J. H.; DeCarlo, P. F.; Allan, J. D.; Coe, H.; Ng, N. L.; Aiken, A. C.; Docherty, K. S.; Ulbrich, I. M.; Grieshop, A. P.; Robinson, A. L.; Duplissy, J.; Smith, J. D.; Wilson, K. R.; Lanz, V. A.; Hueglin, C.; Sun, Y. L.; Tian, J.; Laaksonen, A.; Raatikainen, T.; Rautiainen, J.; Vaattovaara, P.; Ehn, M.; Kulmala, M.; Tomlinson, J. M.; Collins, D. R.; Cubison, M. J.; Dunlea, E. J.; Huffman, J. A.; Onasch, T. B.; Alfarra, M. R.; Williams, P. I.; Bower, K.; Kondo, Y.; Schneider, J.; Drewnick, F.; Borrmann, S.; Weimer, S.; Demerjian, K.; Salcedo, D.; Cottrell, L.; Griffin, R.; Takami, A.; Miyoshi, T.; Hatakeyama, S.; Shimono, A.; Sun, J. Y.; Zhang, Y. M.; Dzepina, K.; Kimmel, J. R.; Sueper, D.; Jayne, J. T.; Herndon, S. C.; Trimborn, A. M.; Williams, L. R.; Wood, E. C.; Middlebrook, A. M.; Kolb, C. E.; Baltensperger, U.; Worsnop, D. R. Evolution of organic aerosols in the atmosphere. *Science* **2009**, *326* (5959), 1525–1529.

(4) Bateman, A. P.; Nizkorodov, S. A.; Laskin, J.; Laskin, A. Time-resolved molecular characterization of limonene/ozone aerosol using high-resolution electrospray ionization mass spectrometry. *Phys. Chem. Chem. Phys.* **2009**, *11* (36), 7931–7942.

(5) Jayne, J. T.; Leard, D. C.; Zhang, X.; Davidovits, P.; Smith, K. A.; Kolb, C. E.; Worsnop, D. R. Development of an aerosol mass spectrometer for size and composition analysis of submicron particles. *Aerosol Sci. Technol.* **2000**, *33* (1–2), 49–70.

(6) DeCarlo, P. F.; Kimmel, J. R.; Trimborn, A.; Northway, M. J.; Jayne, J. T.; Aiken, A. C.; Gonin, M.; Fuhrer, K.; Horvath, T.; Docherty, K. S.; Worsnop, D. R.; Jimenez, J. L. Field-deployable, high-resolution, time-of-flight aerosol mass spectrometer. *Anal. Chem.* **2006**, *78* (24), 8281–8289.

(7) DeCarlo, P. F.; Dunlea, E. J.; Kimmel, J. R.; Aiken, A. C.; Sueper, D.; Crounse, J.; Wennberg, P. O.; Emmons, L.; Shinzuka, Y.; Clarke, A.; Zhou, J.; Tomlinson, J.; Collins, D. R.; Knapp, D.; Weinheimer, A. J.; Montzka, D. D.; Campos, T.; Jimenez, J. L. Fast airborne aerosol size and chemistry measurements above Mexico City and Central Mexico during the MILAGRO campaign. *Atmos. Chem. Phys.* **2008**, *8* (14), 4027–4048.

(8) Shilling, J. E.; Chen, Q.; King, S. M.; Rosenoern, T.; Kroll, J. H.; Worsnop, D. R.; DeCarlo, P. F.; Aiken, A. C.; Sueper, D.; Jimenez, J. L.; Martin, S. T. Loading-dependent elemental composition of alpha-pinene SOA particles. *Atmos. Chem. Phys.* **2009**, *9* (3), 771–782.

(9) Aiken, A. C.; DeCarlo, P. F.; Kroll, J. H.; Worsnop, D. R.; Huffman, J. A.; Docherty, K. S.; Ulbrich, I. M.; Mohr, C.; Kimmel, J. R.; Sueper, D.; Sun, Y.; Zhang, Q.; Trimborn, A.; Northway, M.; Ziemann, P. J.; Canagaratna, M. R.; Onasch, T. B.; Alfarra, M. R.; Prevot, A. S. H.; Dommen, J.; Duplissy, J.; Metzger, A.; Baltensperger, U.; Jimenez, J. L. O/C and OM/OC ratios of primary, secondary, and ambient organic aerosols with high-resolution time-of-flight aerosol mass spectrometry. *Environ. Sci. Technol.* **2008**, *42* (12), 4478–4485.

(10) Aiken, A. C.; DeCarlo, P. F.; Jimenez, J. L. Elemental analysis of organic species with electron ionization high-resolution mass spectrometry. *Anal. Chem.* **2007**, *79* (21), 8350–8358.

(11) Heaton, K. J.; Sleighter, R. L.; Hatcher, P. G.; Hall, W. A.; Johnston, M. V. Composition domains in monoterpene secondary organic aerosol. *Environ. Sci. Technol.* **2009**, *43* (20), 7797–7802.

(12) Schmitt-Kopplin, P.; Gelencser, A.; Dabek-Zlotorzynska, E.; Kiss, G.; Hertkorn, N.; Harir, M.; Hong, Y.; Gebefugi, I. Analysis of the unresolved organic fraction in atmospheric aerosols with ultrahigh-resolution mass spectrometry and nuclear magnetic resonance spectroscopy: Organosulfates as photochemical smog constituents. *Anal. Chem.* **2010**, *82* (19), 8017–8026.

(13) Wozniak, A. S.; Bauer, J. E.; Sleighter, R. L.; Dickhut, R. M.; Hatcher, P. G. Technical note: Molecular characterization of aerosol-derived water soluble organic carbon using ultrahigh resolution electrospray ionization Fourier transform ion cyclotron resonance mass spectrometry. *Atmos. Chem. Phys.* **2008**, *8* (17), 5099–5111.

(14) Altieri, K. E.; Turpin, B. J.; Seitzinger, S. P. Oligomers, organosulfates, and nitrooxy organosulfates in rainwater identified by

ultra-high resolution electrospray ionization FT-ICR mass spectrometry. *Atmos. Chem. Phys.* **2009**, *9* (7), 2533–2542.

(15) Mazzoleni, L. R.; Ehrmann, B. M.; Shen, X. H.; Marshall, A. G.; Collett, J. L. Water-soluble atmospheric organic matter in fog: Exact masses and chemical formula identification by ultrahigh-resolution Fourier transform ion cyclotron resonance mass spectrometry. *Environ. Sci. Technol.* **2010**, *44* (10), 3690–3697.

(16) Laskin, A.; Smith, J. S.; Laskin, J. Molecular characterization of nitrogen-containing organic compounds in biomass burning aerosols using high-resolution mass spectrometry. *Environ. Sci. Technol.* **2009**, *43* (10), 3764–3771.

(17) Smith, J. S.; Laskin, A.; Laskin, J. Molecular characterization of biomass burning aerosols using high-resolution mass spectrometry. *Anal. Chem.* **2009**, *81* (4), 1512–1521.

(18) Chang-Graham, A. L.; Profeta, L. T. M.; Johnson, T. J.; Yokelson, R. J.; Laskin, A.; Laskin, J. Case study of water-soluble metal containing organic constituents of biomass burning aerosol. *Environ. Sci. Technol.* **2011**, *45* (4), 1257–1263.

(19) Bateman, A. P.; Nizkorodov, S. A.; Laskin, J.; Laskin, A. High-resolution electrospray ionization mass spectrometry analysis of water-soluble organic aerosols collected with a particle into liquid sampler. *Anal. Chem.* **2010**, *82* (19), 8010–8016.

(20) Bateman, A. P.; Walsler, M. L.; Desyaterik, Y.; Laskin, J.; Laskin, A.; Nizkorodov, S. A. The effect of solvent on the analysis of secondary organic aerosol using electrospray ionization mass spectrometry. *Environ. Sci. Technol.* **2008**, *42* (19), 7341–7346.

(21) Nguyen, T. B.; Bateman, A. P.; Bones, D. L.; Nizkorodov, S. A.; Laskin, J.; Laskin, A. High-resolution mass spectrometry analysis of secondary organic aerosol generated by ozonolysis of isoprene. *Atmos. Environ.* **2010**, *44* (8), 1032–1042.

(22) Reinhardt, A.; Emmenegger, C.; Gerrits, B.; Panse, C.; Dommen, J.; Baltensperger, U.; Zenobi, R.; Kalberer, M. Ultrahigh mass resolution and accurate mass measurements as a tool to characterize oligomers in secondary organic aerosols. *Anal. Chem.* **2007**, *79* (11), 4074–4082.

(23) Walsler, M. L.; Desyaterik, Y.; Laskin, J.; Laskin, A.; Nizkorodov, S. A. High-resolution mass spectrometric analysis of secondary organic aerosol produced by ozonation of limonene. *Phys. Chem. Chem. Phys.* **2008**, *10* (7), 1009–1022.

(24) Schug, K.; McNair, H. M. Adduct formation in electrospray ionization mass spectrometry II. Benzoic acid derivatives. *J. Chromatogr. A* **2003**, *985* (1–2), 531–539.

(25) Bones, D. L.; Henriksen, D. K.; Mang, S. A.; Gonsior, M.; Bateman, A. P.; Nguyen, T. B.; Cooper, W. J.; Nizkorodov, S. A. Appearance of strong absorbers and fluorophores in limonene-O₃ secondary organic aerosol due to NH₄⁺-mediated chemical aging over long time scales. *J. Geophys. Res., [Atmos.]* **2010**, *115*.

(26) Bateman, A. P.; Nizkorodov, S. A.; Laskin, J.; Laskin, A. Photolytic processing of secondary organic aerosols dissolved in cloud droplets. *Phys. Chem. Chem. Phys.* **2011**, *13* (26), 12199–12212.

(27) Kebarle, P. A brief overview of the present status of the mechanisms involved in electrospray mass spectrometry. *J. Mass Spectrom.* **2000**, *35* (7), 804–817.

(28) Cech, N. B.; Enke, C. G. Practical implications of some recent studies in electrospray ionization fundamentals. *Mass Spectrom. Rev.* **2001**, *20* (6), 362–387.

(29) Oss, M.; Krueve, A.; Herodes, K.; Leito, I. Electrospray ionization efficiency scale of organic compounds. *Anal. Chem.* **2010**, *82* (7), 2865–2872.

(30) Cech, N. B.; Enke, C. G. Relating electrospray ionization response to nonpolar character of small peptides. *Anal. Chem.* **2000**, *72* (13), 2717–2723.

(31) Chalcraft, K. R.; Lee, R.; Mills, C.; Britz-McKibbin, P. Virtual quantification of metabolites by capillary electrophoresis-electrospray ionization-mass spectrometry: predicting ionization efficiency without chemical standards. *Anal. Chem.* **2009**, *81* (7), 2506–2515.

(32) Ehrmann, B. M.; Henriksen, T.; Cech, N. B. Relative importance of basicity in the gas phase and in solution for determining selectivity

in electrospray ionization mass spectrometry. *J. Am. Soc. Mass Spectrom.* **2008**, *19* (5), 719–728.

(33) Koster, S.; Mulder, B.; Duursma, M. C.; Boon, J. J.; Philipsen, H. J. A.; von Velde, J. W.; Nielen, M. W. F.; de Koster, C. G.; Heeren, R. M. A. Quantitative analysis of copolymers: Influence of the structure of the monomer on the ionization efficiency in electrospray ionization FTMS. *Macromolecules* **2002**, *35* (13), 4919–4928.

(34) Mohamed, S.; Charles, L. Selectivity of electrospray response in small polymer analysis by mass spectrometry. *Rapid Commun. Mass Spectrom.* **2006**, *20* (21), 3188–3192.

(35) Tang, L.; Kebarle, P. Dependence of ion intensity in electrospray mass-spectrometry on the concentration of the analytes in the electrosprayed solution. *Anal. Chem.* **1993**, *65* (24), 3654–3668.

(36) Amad, M. H.; Cech, N. B.; Jackson, G. S.; Enke, C. G. Importance of gas-phase proton affinities in determining the electrospray ionization response for analytes and solvents. *J. Mass Spectrom.* **2000**, *35* (7), 784–789.

(37) Henriksen, T.; Juhler, R. K.; Svensmark, B.; Cech, N. B. The relative influences of acidity and polarity on responsiveness of small organic molecules to analysis with negative ion electrospray ionization mass spectrometry (ESI-MS). *J. Am. Soc. Mass Spectrom.* **2005**, *16* (4), 446–455.

(38) Kippenberger, M.; Winterhalter, R.; Moortgat, G. K. Determination of higher carboxylic acids in snow samples using solid-phase extraction and LC/MS-TOF. *Anal. Bioanal. Chem.* **2008**, *392* (7–8), 1459–1470.

(39) Rostad, C. E.; Leenheer, J. A. Factors that affect molecular weight distribution of Suwannee River fulvic acid as determined by electrospray ionization/mass spectrometry. *Anal. Chim. Acta* **2004**, *523* (2), 269–278.

(40) Schug, K.; McNair, H. M. Adduct formation in electrospray ionization. Part 1: Common acidic pharmaceuticals. *J. Sep. Sci.* **2002**, *25* (12), 760–766.

(41) Enke, C. G. A predictive model for matrix and analyte effects in electrospray ionization of singly-charged ionic analytes. *Anal. Chem.* **1997**, *69* (23), 4885–4893.

(42) Gao, Y. Q.; Hall, W. A.; Johnston, M. V. Molecular composition of monoterpene secondary organic aerosol at low mass loading. *Environ. Sci. Technol.* **2010**, *44* (20), 7897–7902.

(43) Hall, W. A.; Johnston, M. V. Oligomer content of alpha-pinene secondary organic aerosol. *Aerosol Sci. Technol.* **2011**, *45* (1), 37–45.

(44) Jang, M.; Kamens, R. M. Newly characterized products and composition of secondary aerosols from the reaction of alpha-pinene with ozone. *Atmos. Environ.* **1999**, *33* (3), 459–474.

(45) Yu, J. Z.; Griffin, R. J.; Cocker, D. R.; Flagan, R. C.; Seinfeld, J. H.; Blanchard, P. Observation of gaseous and particulate products of monoterpene oxidation in forest atmospheres. *Geophys. Res. Lett.* **1999**, *26* (8), 1145–1148.

(46) Glasius, M.; Lahaniati, M.; Calogirou, A.; Di Bella, D.; Jensen, N. R.; Hjorth, J.; Kotzias, D.; Larsen, B. R. Carboxylic acids in secondary aerosols from oxidation of cyclic monoterpenes by ozone. *Environ. Sci. Technol.* **2000**, *34* (6), 1001–1010.

(47) Heaton, K. J.; Dreyfus, M. A.; Wang, S.; Johnston, M. V. Oligomers in the early stage of biogenic secondary organic aerosol formation and growth. *Environ. Sci. Technol.* **2007**, *41* (17), 6129–6136.

(48) Chen, Q.; Liu, Y. J.; Donahue, N. M.; Shilling, J. E.; Martin, S. T. Particle-phase chemistry of secondary organic material: modeled compared to measured O:C and H:C elemental ratios provide constraints. *Environ. Sci. Technol.* **2011**, *45* (11), 4763–4770.

(49) *CRC Handbook of Chemistry and Physics*, 81st ed.; Lide, D. R., Ed.; CRC Press: Boca Raton, FL, 2000; pp 16–43.

(50) Leungskul, S.; Jaoui, M.; Kamens, R. M. Kinetic mechanism for predicting secondary organic aerosol formation from the reaction of *d*-limonene with ozone. *Environ. Sci. Technol.* **2005**, *39* (24), 9583–9594.

(51) Mopper, K.; Stubbins, A.; Ritchie, J. D.; Bialk, H. M.; Hatcher, P. G. Advanced instrumental approaches for characterization of marine dissolved organic matter: Extraction techniques, mass spectrometry,

and nuclear magnetic resonance spectroscopy. *Chem. Rev.* **2007**, *107* (2), 419–442.

(52) Lin, P.; Rincon, A. g.; Kalberer, M.; Yu, J. Z. Elemental composition of HULIS in the Pearl River Delta Region, China: Results inferred from positive and negative electrospray high resolution mass spectrometric data. *Environ. Sci. Technol.* **2012**, in press.

(53) Nizkorodov, S. A.; Laskin, J.; Laskin, A. Molecular chemistry of organic aerosols through the application of high resolution mass spectrometry. *Phys. Chem. Chem. Phys.* **2011**, *13* (9), 3612–3629.

(54) Chen, X.; Hopke, P. K.; Carter, W. P. L. Secondary organic aerosol from ozonolysis of biogenic volatile organic compounds: Chamber studies of particle and reactive oxygen species formation. *Environ. Sci. Technol.* **2011**, *45* (1), 276–282.